PHENOMENOLOGY OF FLAVOR SYMMETRIES: AN EXAMPLE*

Janusz Gluza, Biswajit Karmakar

Institute of Physics, University of Silesia, Katowice, Poland

Received 1 June 2025, accepted 9 December 2025, published online 19 December 2025

We undertake the issue of flavor symmetries in the context of lepton masses and mixing which can lead to possible signatures in the current and future experiments at the intensity, energy, and cosmic frontiers. Giving an example of the A_4 discrete symmetry, we show how to construct corresponding neutrino mass terms, leading to neutrino mass and mixing matrices with suitable correlations between parameters and unique phenomenological predictions.

DOI:10.5506/APhysPolBSupp.18.6-A20

1. Introduction

Within the known Pontecorvo–Maki–Nakagawa–Sakata parametrization of the mixing matrix U [1–3], we have three mixing angles: θ_{12}, θ_{23}, and θ_{13}, and the Dirac CP-violating phase $\delta_{\rm CP}$ (oscillation experiments are not sensitive to two Majorana phases). The remaining two parameters are mass squared differences which are connected with solar and atmospheric neutrino oscillations: $\Delta m^2_\odot = m_2^2 - m_1^2$, $\Delta m^2_A = |m_3^2 - m_1^2|$.

The current main questions in neutrino oscillation physics are:

(i) What is the mass ordering of the neutrinos (*i.e.* sign of $|\Delta m^2_{32(1)}|$)?

(ii) What is the octant of θ_{23}?

(iii) Is the CP symmetry violated in neutrino oscillations? (Non-zero $\delta_{\rm CP}$ phase).

Hence, still ambiguities are seen over 3 parameters, $|\Delta m^2_{32(1)}|$, θ_{23}, and $\delta_{\rm CP}$.

One more frequently posed question is what kind of symmetry can be responsible for different values of mixing angles and masses. For normal mass

* Presented at the V4-HEP 4 — Theory and Experiment in High Energy Physics Workshop, Warsaw, Poland, 28–31 October, 2024.

ordering, based on the present NuFIT-6.0 global analysis [4], the central values of neutrino parameters are

$$\begin{aligned} \Delta m^2_{21} &= 7.49\times 10^{-5}\ \mathrm{eV}^2\,, \qquad |\Delta m^2_{31}| = 2.513\times 10^{-3}\ \mathrm{eV}^2\,,\\ \sin^2\theta_{12} &= 0.308\,, \qquad \sin^2\theta_{23} = 0.47\,, \qquad \sin^2\theta_{13} = 0.02215\,,\\ \delta_{\mathrm{CP}} &= 212^{\circ}{}^{+26^{\circ}}_{-41^{\circ}}\,. \end{aligned} \tag{1}$$

There are essentially three main directions towards understanding neutrino mixing structure and mass spectrum: anarchy, textures, and symmetries. In the anarchy hypothesis [5–8], the leptonic mixing matrix manifests as a random draw from an unbiased distribution of unitary 3×3 matrices and does not point towards any principle or its origin. This hypothesis does not make any correlation between the neutrino masses and mixing parameters. However, it predicts a probability distribution for the parameters which parameterize the mixing matrix. Though random matrices cannot solve fundamental problems in neutrino physics, they generate intriguing hints on the nature of neutrino mass matrices. In the texture approach, some zeros of neutrino mass matrices can be eliminated. More details on this approach can be found in [9].

Here, we will concentrate on flavor discrete symmetries which are able to explain the structure of unitary neutrino mixings[1] and masses. This is a very broad subject, treated recently in a review [9], where, in addition, phenomenological aspects of such models have been discussed. In general, flavor discrete symmetries can be tested at intensity and energy frontier experiments, as well as the cosmic frontier. In this short note, we pick up one representative example of how a model with given flavor symmetry is constructed to satisfy data in Eq. (1) and show a phenomenological example of how the model can be tested at one of the mentioned frontiers.

2. Matching A_4 discrete group to neutrino mixing and masses

The neutrino mixing matrix U between massive and weak neutrino states $|\nu^{(f)}_\alpha\rangle = \sum_{i=1}^{3} (U)_{\alpha i}\, |\nu^{(m)}_i\rangle$ fits well to the so-called tribimaximal mixing [14, 15]

$$U_{\mathrm{TBM}} = \begin{pmatrix} \sqrt{\frac{2}{3}} & \frac{1}{\sqrt{3}} & 0 \\ -\frac{1}{\sqrt{6}} & \frac{1}{\sqrt{3}} & -\frac{1}{\sqrt{2}} \\ -\frac{1}{\sqrt{6}} & \frac{1}{\sqrt{3}} & \frac{1}{\sqrt{2}} \end{pmatrix}. \tag{2}$$

[1] In [10], the neutrino mixing matrix is described using singular values which can, in addition, cover non-unitary effects and the issue of the number of additional right-handed neutrinos and light–heavy mixings [11]. For more on non-unitary effects, see [12], and in the context of discrete symmetries [13].

It appears that the zero element in the above matrix is experimentally small, so U_{TBM} must be modified. Anyway, the neutrino mixing matrix has a special structure which we would like to understand in terms of some underlying symmetry. Here, we will show the case of A_4 discrete symmetry which is used to construct the appropriate Yukawa couplings leading to the neutrino mass matrix. The unphysical (non-diagonal) mass matrix can be diagonalized to the physical massive states restoring the structure of neutrino mixings. This is the first step. In the next step, we choose which column of the original TBM mixing we would like to be kept unchanged, thus we consider TM_1 and TM_2 mixing schemes in which columns 1 and 2 in Eq. (2) remain unchanged, respectively. For step 1, we use the group A_4, an alternating group of order 4, *i.e.*, the group of even permutations of four objects. It has 12 elements and is the smallest non-Abelian group with a triplet irreducible representation, making it ideal for models with three generations of fermions. Geometrically, it is a symmetry group of a tetrahedron, like for a diamond, see Fig. 1.

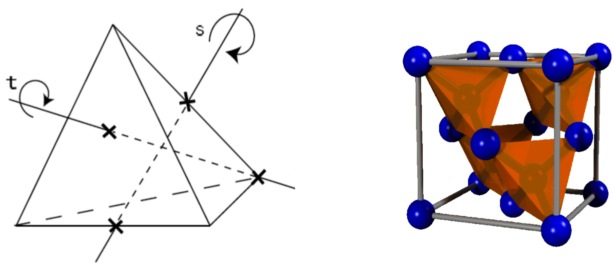

Fig. 1. A_4 symmetry as a tetrahedron and the diamond lattice. The diamond lattice structure is a specific arrangement of carbon atoms in a crystalline form, exhibiting remarkable symmetry and unique physical properties. One interesting aspect of this structure is its connection to the mathematical concept of A_4 symmetry, which can be understood through group theory. The diamond lattice is a variation of the face-centered cubic (FCC) structure. Each carbon atom in a diamond lattice is tetrahedrally coordinated, bonded to four other carbon atoms. Figure source: Wikipedia and P. Kuiper.

For a detailed discussion on A_4 character table and three-dimensional unitary representation of the generators, see Refs. [16, 17]. Two generators, known as S and T, can form all the 12 elements (through multiplications in all possible ways) which obey the relation

$$S^2 = T^3 = (ST)^3 = 1\,. \tag{3}$$

This relation dictates the 'presentation' of the group. Therefore, the three 1-dimensional representations are given by

$$1 \to (S=1, T=1)\,, \qquad 1' \to (S=1, T=\omega)\,, \qquad 1'' \to \left(S=1, T=\omega^2\right)\,, \tag{4}$$

where $\omega = \mathrm{e}^{2i\pi/3}$ is a cubic root of unity. Now, the basis for the 3-dimensional representation is written as

$$S = \frac{1}{3}\begin{pmatrix} -1 & 2 & 2 \\ 2 & -1 & 2 \\ 2 & 2 & -1 \end{pmatrix}\,, \qquad T = \begin{pmatrix} 1 & 0 & 0 \\ 0 & \omega & 0 \\ 0 & 0 & \omega^2 \end{pmatrix}\,, \tag{5}$$

from which all 12 matrices of the 3-dimensional representation of A_4 can be obtained. Alternatively, S, T can be written in another 3-dimensional unitary representation, where S is diagonal. The equivalence between these two bases and its effect on the relative phases of the neutrino mass eigenvalues has been discussed in [18].

The multiplication rules of the singlets and triplets are given by [16, 17]

$$\begin{aligned} 1 \otimes 1 &= 1\,, \qquad 1' \otimes 1'' = 1\,, \qquad 1' \otimes 1' = 1''\,, \qquad 1'' \otimes 1'' = 1'\,, \\ 3 \otimes 3 &= 1 \oplus 1' \oplus 1'' \oplus 3_{\mathrm{s}} \oplus 3_{\mathrm{a}}\,, \end{aligned} \tag{6}$$

where the subscripts "s" and "a" denote symmetric and antisymmetric parts respectively. In the T diagonal basis [16], writing two triplets as (x_1, x_2, x_3) and (y_1, y_2, y_3), respectively, we can write their products explicitly as

$$\begin{aligned} 1 &\sim x_1y_1 + x_2y_3 + x_3y_2\,, \\ 1' &\sim x_3y_3 + x_1y_2 + x_2y_1\,, \\ 1'' &\sim x_2y_2 + x_1y_3 + x_3y_1\,, \\ 3_{\mathrm{s}} &\sim \frac{1}{3}\begin{pmatrix} 2x_1y_1 - x_2y_3 - x_3y_2 \\ 2x_3y_3 - x_1y_2 - x_2y_1 \\ 2x_2y_2 - x_1y_3 - x_3y_1 \end{pmatrix}\,, \qquad 3_{\mathrm{a}} \sim \frac{1}{2}\begin{pmatrix} x_2y_3 - x_3y_2 \\ x_1y_2 - x_2y_1 \\ x_3y_1 - x_1y_3 \end{pmatrix}\,. \end{aligned} \tag{7}$$

Here, we show how to use these multiplication rules for A_4 applied to be a symmetry in the neutrino sector. This symmetry in the Lagrangian can explain the observed neutrino mixing. The complete Lagrangian is discussed in [19]. For illustration, we consider one chosen piece of the Lagrangian for neutrino mass contributions in the so-called FSS (flavor–scoto–seesaw) model ('skótos' from Greek means 'darkness')

$$\mathcal{L} = \frac{y_N}{\Lambda}\left(\bar{L}\phi_S\right)_1 \tilde{H} N_{\mathrm{R}} + \mathrm{h.c.}\,, \tag{8}$$

where y_N is the coupling constant and N_{R} is the right-handed Majorana neutrino. The SM lepton doublet L (A_4 triplet) contracts with the so-called 'flavon' scalar field ϕ_S (also triplet) giving representation 1 of A_4 in (7). Taking flavon fields get VEVs along $\langle\phi_S\rangle = (0, v_s, -v_s)$, the A_4 flavor decomposition for the contribution to the neutrino sector in accordance with (7) can be written as

$$\mathcal{L} = \frac{y_N}{\Lambda}\left(\bar{L}_1\phi_{S_1} + \bar{L}_2\phi_{S_3} + \bar{L}_3\phi_{S_2}\right)\tilde{H}N_\mathrm{R} = \frac{y_N}{\Lambda}\left(\bar{L}_2 v_s - \bar{L}_3 v_s\right)\tilde{H}N_\mathrm{R} + \text{h.c.} \tag{9}$$

Assuming two RHNs (considering the minimal seesaw scenario for the type-I contribution), with additional flavon ϕ_A and $\langle\phi_A\rangle = (v_a, v_a, v_a)$, we get the Dirac neutrino mass matrix

$$M_\mathrm{D} = \frac{v}{\Lambda}\begin{pmatrix} 0 & y_{N_2}v_a \\ -y_{N_1}v_s & y_{N_2}v_a \\ y_{N_1}v_s & y_{N_2}v_a \end{pmatrix} = vY_N\,, \qquad M_\mathrm{R} = \begin{pmatrix} M_{N_1} & 0 \\ 0 & M_{N_2} \end{pmatrix}. \tag{10}$$

In the next step, we add small 1-loop mass contributions allowing in the final accord for the small deviations from the TBM scheme. This additional mass term helps to explain the ratio of solar to atmospheric mass difference

$$r = \frac{\Delta m^2_\mathrm{SOL}}{\Delta m^2_\mathrm{ATM}} \simeq \frac{7.41\times10^{-5}\ \mathrm{eV}^2}{2.51\times10^{-3}\ \mathrm{eV}^2} \simeq 3\times10^{-2}\,. \tag{11}$$

The 1-loop mass term is introduced with an effective interaction of fermion f, SU(2) scalar soublet η, A_4 flavon ϕ_S (triplet), and ξ (singlet) at dim-6: $\mathcal{L}_\mathrm{LOOP} = \frac{y_s}{\Lambda^2}(\bar{L}\phi_S)\xi i\sigma_2\eta^* f + \frac{1}{2}M_f\bar{f}^c f + \text{h.c.}$, where $\langle\phi_S\rangle = (0, v_s, -v_s)$, $\langle\xi\rangle = v_\xi$, leading to the mass term $(M_\nu)_\mathrm{LOOP} = \mathcal{F}(m_{\eta_R}, m_{\eta_I}, M_f)M_f Y_f^i Y_f^j$ with couplings depending on flavons VEVs $Y_F = (Y_F^e, Y_F^\mu, Y_F^\tau)^T = (y_s\frac{v_s}{\Lambda}\frac{v_\xi}{\Lambda}, 0, -y_s\frac{v_s}{\Lambda}\frac{v_\xi}{\Lambda})^T$. Here, $\mathcal{F}(m_{\eta_R}, m_{\eta_I}, M_f)$ is the loop function, M_{η_R} and M_{η_I} are the masses of the neutral component of η.

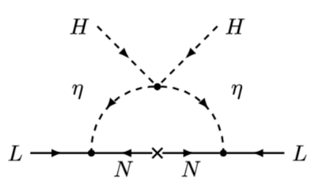

Fig. 2. Generation of the small 1-loop mass term.

Therefore, the corresponding mass matrix takes the form

$$(M_\nu)_\mathrm{LOOP} = C\begin{pmatrix} 1 & 0 & -1 \\ 0 & 0 & 0 \\ -1 & 0 & 1 \end{pmatrix}, \qquad C = \mathcal{F}(m_{\eta_R}, m_{\eta_I}, M_f)y_s^2\frac{v_s^2 v_\xi^2}{\Lambda^4}\,. \tag{12}$$

Here, $\mathcal{F}(m_{\eta_R}, m_{\eta_I}, M_f)$ is the loop function and the effective neutrino mass matrix is

$$
\begin{aligned}
M_\nu &= -M_{\rm D} M_{\rm R}^{-1} M_{\rm D}^T + (M_\nu)_{\rm LOOP} = (M_\nu)_{\rm TREE} + (M_\nu)_{\rm LOOP} \\
&= \begin{pmatrix} -B+C & -B & -B-C \\ -B & -A-B & A-B \\ -B-C & A-B & -A-B+C \end{pmatrix} , \\
A &= \frac{v^2 v_s^2 y_{N_1}^2}{\Lambda^2 M_{N_1}} , \qquad B = \frac{v^2 v_a^2 y_{N_2}^2}{\Lambda^2 M_{N_2}} . \qquad (13)
\end{aligned}
$$

Note that A, B elements are suppressed by Λ^2, while C is suppressed by Λ^4 (1-loop effect). After rotation by the TBM matrix

$$
M'_\nu = U_{\rm TBM}^T M_\nu U_{\rm TBM} = \frac{1}{2} \begin{pmatrix} 3C & 0 & -\sqrt{3}C \\ 0 & -6B & 0 \\ -\sqrt{3}C & 0 & -4A+C \end{pmatrix} , \qquad (14)
$$

we arrive at the effective neutrino mixing matrix (TM_2 mixing [19])

$$
U_\nu = U_{\rm TBM} U_{13} = \begin{pmatrix} \sqrt{\frac{2}{3}}\cos\theta & \frac{1}{\sqrt{3}} & \sqrt{\frac{2}{3}}\,{\rm e}^{i\phi}\sin\theta \\ -\frac{\cos\theta}{\sqrt{6}} + \frac{{\rm e}^{i\phi}\sin\theta}{\sqrt{2}} & \frac{1}{\sqrt{3}} & -\frac{\cos\theta}{\sqrt{2}} - \frac{{\rm e}^{i\phi}\sin\theta}{\sqrt{6}} \\ -\frac{\cos\theta}{\sqrt{6}} - \frac{{\rm e}^{i\phi}\sin\theta}{\sqrt{2}} & \frac{1}{\sqrt{3}} & \frac{\cos\theta}{\sqrt{2}} - \frac{{\rm e}^{i\phi}\sin\theta}{\sqrt{6}} \end{pmatrix} U_m . \qquad (15)
$$

U_m stays for possible Majorana CP-phases, U_{13} is the standard Euler rotation matrix around the y-axis. Comparing the above mixing matrix with the standard $U_{\rm PMNS}$, we get correlations between TM_2 parameters

$$
\sin\theta_{13}\,{\rm e}^{-i\delta_{\rm CP}} = \sqrt{\frac{2}{3}}\,{\rm e}^{-i\phi}\sin\theta , \qquad \tan^2\theta_{12} = \frac{1}{2-3\sin^2\theta_{13}} , \qquad (16)
$$

$$
\tan^2\theta_{23} = \frac{\left(1 + \frac{\sin\theta_{13}\cos\phi}{\sqrt{2-3\sin^2\theta_{13}}}\right)^2 + \frac{\sin^2\theta_{13}\sin^2\phi}{(2-3\sin^2\theta_{13})}}{\left(1 - \frac{\sin\theta_{13}\cos\phi}{\sqrt{2-3\sin^2\theta_{13}}}\right)^2 + \frac{\sin^2\theta_{13}\sin^2\phi}{(2-3\sin^2\theta_{13})}} . \qquad (17)
$$

3. Phenomenological predictions

The phenomenology of such models like TM_2 is very rich [9, 19]. Here, we give only an example of constraints on parameters coming from correlations like in (16), (17), and from low-energy LFV neutrinoless double beta decay process.

In Fig. 3, we show two numerical examples of phenomenological predictions for the described TM_2 model. It is evident from the top plot that only the higher octant of θ_{23} is favored (*i.e.* $\theta_{23} \geq 45°$) in the considered TM_2 model. Furthermore, the cyan patch represents the disallowed region for δ_{CP} in order to satisfy the limits on light neutrino masses [20]. The allowed regions for the Dirac CP phase δ_{CP} are given by $-1.57 \leq \delta_{\mathrm{CP}} \leq 1.37$ and $1.4 \leq \delta_{\mathrm{CP}} \leq 1.57$ for NH.

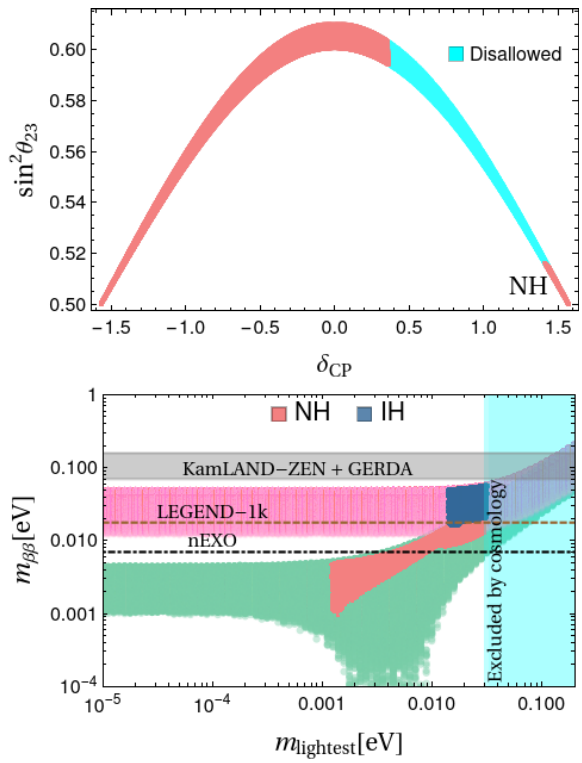

Fig. 3. Top: Correlation between $\sin^2\theta_{23}$ and δ_{CP} for NH. The cyan region is excluded by light neutrino mass constraints. Bottom: $m_{\beta\beta}$ *versus* lightest neutrino mass for NH (light red) and IH (blue). Green/magenta: 3σ-allowed regions. Gray, brown dashed, and black dot-dashed lines: limits from KamLAND-Zen+GERDA, LEGEND-1k, and nEXO. Cyan band: cosmologically excluded.

The bottom plot in Fig. 3 shows the effective mass parameter characterizing neutrinoless double beta decay ($m_{\beta\beta}$) against the lightest neutrino mass for both NH and IH. The predictions for $m_{\beta\beta}$ are 1–30 meV for NH and 16–60 meV for IH. The green and magenta shaded regions represent 3σ allowed regions for the $m_{\beta\beta}$ predictions for NH and IH, respectively. The vertical cyan-shaded regions represent the cosmological upper limit on the sum of absolute neutrino masses. The gray shaded region represents the upper limit for $m_{\beta\beta}$ by combined analysis of KamLAND-Zen [21] and GERDA [22] experiments and predictions for $m_{\beta\beta}$ in the TM_2 model fall within this upper limit. The brown dashed and black dot-dashed lines stand for future sensitivities of the LEGEND-1k [23] and nEXO [24] experiments, respectively. Thus, these near-future experiments have the potential to almost entirely falsify the IH prediction and probe a major part of the prediction for $m_{\beta\beta}$ for NH of light neutrino mass.

4. Conclusions

Is there any guiding principle behind the observed pattern of lepton mixing? (Discrete) flavor symmetry is one such potential candidate where tiny neutrino mass may originate from hybrid scoto–seesaw scenarios. It explains the hierarchy of the mass scales involved in neutrino oscillation, neutrino mixing angles and predicts strict ranges of CP phases, leading to many phenomenological predictions at intensity, energy and cosmology frontiers [9]. In the proceedings, we have shown how a specific Lagrangian term can be introduced for the purpose of specific phenomenological studies with some correlations among neutrino mass and mixing parameters leading to unique predictions, here on the neutrinoless double beta decay.

This work has been supported in part by the National Science Center, Poland (NCN) under grant No. 2020/37/B/ST2/02371.

REFERENCES

[1] B. Pontecorvo, *Zh. Eksp. Teor. Fiz.* **34**, 247 (1957).

[2] Z. Maki, M. Nakagawa, S. Sakata, *Prog. Theor. Phys.* **28**, 870 (1962).

[3] M. Kobayashi, T. Maskawa, *Prog. Theor. Phys.* **49**, 652 (1973).

[4] I. Esteban *et al.*, *J. High Energy Phys.* **2024**, 216 (2024), arXiv:2410.05380 [hep-ph].

[5] L.J. Hall, H. Murayama, N. Weiner, *Phys. Rev. Lett.* **84**, 2572 (2000), arXiv:hep-ph/9911341.

[6] A. de Gouvea, H. Murayama, *Phys. Lett. B* **747**, 479 (2015), arXiv:1204.1249 [hep-ph].

[7] N. Haba, H. Murayama, *Phys. Rev. D* **63**, 053010 (2001), arXiv:hep-ph/0009174.

[8] J. Gluza, R. Szafron, *Phys. Rev. D* **85**, 047701 (2012), arXiv:1111.7278 [hep-ph].

[9] G. Chauhan *et al.*, *Prog. Part. Nucl. Phys.* **138**, 104126 (2024), arXiv:2310.20681 [hep-ph].

[10] K. Bielas, W. Flieger, J. Gluza, M. Gluza, *Phys. Rev. D* **98**, 053001 (2018), arXiv:1708.09196 [hep-ph].

[11] W. Flieger, J. Gluza, K. Porwit, *J. High Energy Phys.* **2020**, 169 (2020), arXiv:1910.01233 [hep-ph].

[12] M. Blennow *et al.*, *Nucl. Phys. B* **1017**, 116944 (2025), arXiv:2502.19480 [hep-ph].

[13] B. Karmakar, A. Sil, *Phys. Rev. D* **96**, 015007 (2017), arXiv:1610.01909 [hep-ph].

[14] P.F. Harrison, D.H. Perkins, W.G. Scott, *Phys. Lett. B* **530**, 167 (2002), arXiv:hep-ph/0202074.

[15] P.F. Harrison, W.G. Scott, *Phys. Lett. B* **535**, 163 (2002), arXiv:hep-ph/0203209.

[16] G. Altarelli, F. Feruglio, *Rev. Mod. Phys.* **82**, 2701 (2010), arXiv:1002.0211 [hep-ph].

[17] H. Ishimori *et al.*, *Prog. Theor. Phys. Suppl.* **183**, 1 (2010), arXiv:1003.3552 [hep-th].

[18] J. Barry, W. Rodejohann, *Phys. Rev. D* **81**, 093002 (2010), arXiv:1003.2385 [hep-ph]; *Erratum ibid.* **81**, 119901 (2010),

[19] J. Ganguly, J. Gluza, B. Karmakar, *J. High Energy Phys.* **2022**, 074 (2022), arXiv:2209.08610 [hep-ph].

[20] P.F. de Salas *et al.*, *J. High Energy Phys.* **2021**, 071 (2021), arXiv:2006.11237 [hep-ph].

[21] A. Gando *et al.*, *Phys. Rev. Lett.* **117**, 082503 (2016), arXiv:1605.02889 [hep-ex]; *Addendum ibid.* **117**, 109903 (2016)

[22] M. Agostini *et al.*, *Phys. Rev. Lett.* **120**, 132503 (2018), arXiv:1803.11100 [nucl-ex].

[23] N. Abgrall *et al.*, arXiv:2107.11462 [physics.ins-det].

[24] G. Adhikari *et al.*, *J. Phys. G: Nucl. Part. Phys.* **49**, 015104 (2022), arXiv:2106.16243 [nucl-ex].